

Article

Nitrogen and Phosphorus Co-Doped Carbon Dots for the Growth Promotion of Water Spinach

Fan Yu ¹, Mengqi She ¹, Xia Cai ¹, Xiaoyan Li ¹, Yuan Huang ^{2,3,4} , Hongwei Lei ^{1,*}  and Zuojun Tan ^{1,3,4,*} ¹ College of Engineering, Huazhong Agricultural University, Wuhan 430070, China² College of Horticulture and Forestry Sciences, Huazhong Agricultural University, Wuhan 430070, China³ Shenzhen Institute of Nutrition and Health, Huazhong Agricultural University, Shenzhen 518000, China⁴ Shenzhen Branch, Guangdong Laboratory for Lingnan Modern Agriculture, Genome Analysis Laboratory of the Ministry of Agriculture, Agricultural Genomics Institute at Shenzhen, Chinese Academy of Agricultural Sciences, Shenzhen 518000, China

* Correspondence: leihw@mail.hzau.edu.cn (H.L.); tzj@mail.hzau.edu.cn (Z.T.)

Abstract: Carbon dots have received much attention due to their unique physicochemical properties and diverse applications in bioimaging, optoelectronic devices, catalysis, and agriculture. Here, in this work, we report a simple hydrothermal synthesis of nitrogen and phosphorus-doped carbon dots (N, P-CDs). The optical and physical properties of the synthesized N, P-CDs are analyzed using systematical spectroscopy and electrical characterization. The synthesized N, P-CDs show strong photoluminescence at 626 nm and demonstrate high stability under UV light and other conditions. Moreover, we incorporate the synthesized N, P-CDs into water spinach by root spraying and leaf spraying. It is found that N, P-CDs could effectively promote the growth of water spinach by accelerating the photosynthetic rate, and increasing the content of total phenols, anthocyanins, and flavonoids in water spinach.

Keywords: nanomaterials; carbon dots; doping; plant growth

Citation: Yu, F.; She, M.; Cai, X.; Li, X.; Huang, Y.; Lei, H.; Tan, Z. Nitrogen and Phosphorus Co-Doped Carbon Dots for the Growth Promotion of Water Spinach. *Symmetry* **2023**, *15*, 1532. <https://doi.org/10.3390/sym15081532>

Academic Editor: Vasilis K. Oikonomou

Received: 5 July 2023

Revised: 28 July 2023

Accepted: 1 August 2023

Published: 3 August 2023



Copyright: © 2023 by the authors. Licensee MDPI, Basel, Switzerland. This article is an open access article distributed under the terms and conditions of the Creative Commons Attribution (CC BY) license (<https://creativecommons.org/licenses/by/4.0/>).

1. Introduction

Vegetables are an important source of natural dietary fiber that can regulate the human intestinal microbiota and ensure human health [1]. Vegetables also contain a large number of trace elements and vitamins required by the human body [2,3]. For example, vegetables are rich in vitamin C [4]. The human body needs a sufficient amount of vitamin C for normal activities, but the human body cannot synthesize it and can only obtain it through external sources [5]. A lack of vitamin C can lead to fatigue, ulcerations, and other symptoms [6]. In recent years, with the long-term heavy use of pesticides and chemical fertilizers, the heavy metals in vegetables have increased substantially [7]. The high level of heavy metals in vegetables not only reduces their nutritional quality but also threatens human health [8]. In addition, many of the crops produced today, while meeting the caloric requirements of the human diet, are unable to meet the corresponding micronutrient requirements, resulting in nutritional deficiencies [9]. It is important to improve the nutritional quality of vegetables considering that they are one of the main sources of nutrition. Therefore, we need a fertilizer that is environmentally friendly and can also improve the production and nutrition of plants.

Carbon dots (CDs) are nanomaterials with a particle size of less than 10 nm [10]. Carbon dots, as a new type of carbon-based material, have significant advantages compared to traditional carbon-based materials [11,12]. For example, CDs have a small particle size, so they can easily enter into the cells of plants and animals. The preparation process of CDs is simple and inexpensive. In addition, many functional groups on the surface of CDs are hydrophilic, so their solid powder has excellent solubility in water [13]. In recent years, CDs have achieved excellent results in plant applications [14]. For example, in 2018, Zhang

et al. synthesized chiral CDs from citric acid and L-cysteine or D-cysteine for the growth phase of mung bean sprouts and found that these asymmetric carbon dots were effective in enhancing plant growth [15]. The CDs also have the function of enhancing crop stress tolerance. In 2018, Su et al. used peanuts as an experimental sample and applied CDs to peanut plants; they then examined the whole life cycle of peanut plants. It was found that CDs can improve peanut growth and also improve peanut stress resistance [16]. Compared with traditional fertilizers such as phosphate fertilizer, CDs can be completely absorbed by the plant and will not exist in the environment [17]. Thus, its impact on the environment is negligible. Furthermore, CDs can accelerate the photosynthesis process in plants [18,19]. These advantages make CDs promising green fertilizers for plants.

In this work, we synthesized N, P-CDs using o-phenylenediamine and phosphoric acid as raw materials by a one-step hydrothermal method. We used N, P-CDs in water spinach to promote its growth and enhance its nutritional quality. N, P-CDs with a gradient of concentrations were applied to the vegetables using leaf spraying and root spraying. The overall indicators such as fresh (dry) weight as well as photosynthetic parameters were systematically evaluated, revealing that N, P-CDs can effectively improve the nutritional quality and growth condition of water spinach.

2. Materials and Methods

2.1. Preparation of N, P-CDs

The N, P-CDs were prepared by a one-pot hydrothermal method using o-phenylenediamine and phosphoric acid. A total of 0.5407 g of o-phenylenediamine and 1 mL of phosphoric acid were mixed and dissolved in 25 mL of deionized water. The mixed solution was transferred to a PTFE-lined reactor and heated at 160 °C. After cooling to an ambient temperature, the obtained solution was transferred to a centrifuge tube, and the crude product was filtered by centrifugation, followed by the removal of large particle residues using a 0.22 µm filter membrane. After dialysis and lyophilization, a solid powder was obtained.

2.2. Characterization of N, P-CDs

The morphology of N, P-CDs was observed using a JEM 2100f electron microscope. The fractions of N, P-CDs were determined using a Fourier Transform infrared spectroscopy (FT-IR) and an EXCLAB 250Xi X-ray photoelectron spectrometer (XPS). UV-vis absorption spectra and fluorescence spectra (PL) was measured using a UV-vis 1800 UV spectrophotometer and an RF-6000 fluorescence spectrometer, respectively.

2.3. Selection and Cultivation of Water Spinach

Full, evenly sized seeds were sown in small polyurethane foam cubes, which were placed in a foam seedling tray and germinated in the dark at 29 °C. The seeds were then planted in the dark. After two days, the seeds showed their whiteness and the seedlings were planted when the cotyledons had spread. The plants were exposed to light in an artificial climate chamber with LED white light at an intensity of 200 µmol/(m²·s) and a photoperiod of 12 h/12 h.

The roots and leaves of water spinach were treated separately, with the two treatment groups experimentally independent and not interfering with each other. Seedlings with flattened leaves and uniform growth were selected for transplanting, and a control group of five treatment groups was set up. N, P-CD powder was dissolved in a hydroponic solution, and the solution was prepared in different concentration gradients (0, 25 mg/L, 50 mg/L, 100 mg/L, 200 mg/L, 400 mg/L). The roots of water spinach were treated with this solution. When using the leaf-spraying method, we dissolved the N, P-CDs in deionized water, configured the same concentration gradient, and sprayed them on water spinach leaves. To prevent the carbon dot solution from falling into the hydroponic solution during spraying, the spraying process was blocked with cut plastic partitions. The cultivation cycle was 20 days, and N, P-CDs were used every 4 days.

2.4. Morphology Determination of Water Spinach

The yield of the plant was the sum of the total amount of stems, leaves, and roots, and the dried fresh matter mass was sampled at the end of that measurement. Plants were washed and dried on absorbent paper and the fresh matter mass of individual stems, leaves, and roots was measured separately. The plants were dried in an oven at 105 °C for 30 min; kept at 75 °C until constant weight; and the dry matter mass of stems, leaves, and roots was measured.

2.5. Determination of Nutritional Quality and Photosynthetic Pigments

The content of total phenols, anthocyanins, and flavonoids was determined according to the method of Cao and coworkers [20]. Chlorophyll was extracted with 95% ethanol and the absorbance at 664 nm, 648 nm, and 470 nm was measured by UV-vis spectrophotometer. Plant photosynthetic parameters including photosynthetic rate (Pn), stomatal conductance (Gs), intercellular CO₂ concentration (Ci), and transpiration rate (Tr) were measured using a portable LI-6400XT photosynthesizer.

2.6. Statistical Analysis

Data were analyzed by ANOVA ($p < 0.05$) using SPSS 23 statistical analysis software, and hypothetical ANOVA tests were performed using the S–N–K method. Plots were drawn using Origin 2019 software. Morphological indicators were repeated six times, and physiological indicators were repeated three times. The results were expressed as mean \pm standard deviation.

3. Results

3.1. Spectroscopic Characterization of N, P-CDs

N, P-CDs show significant fluorescence emission under 510–650 nm excitation (Figure 1a). With increasing excitation wavelengths, N, P-CDs show excellent red light emissions at different excitation wavelengths. The maximum fluorescence intensity is at an excitation of 610 nm, corresponding to an emission wavelength of 626 nm, with a shoulder peak at around 675 nm. The N, P-CD solution appears pale yellow under daily light and bright red fluorescence under UV (530 nm) irradiation. N, P-CDs have two peaks at 282 nm and 450 nm (Figure 1b), where the absorption peak at 282 nm is a π – π^* leap in the C=C bond in the aromatic ring, and the absorption peak at 450 nm is attributed to the n – π^* leap in the C=O bond and the π – π^* leap in the aromatic fluorophore structure [21].

Figure 1c,d show the spherical shape and good dispersion of the N, P-CDs, and the HRTEM illustrates the distinct lattice striations of the N, P-CDs. The calculated crystal plane spacing is 0.21 nm, which is consistent with the (100) crystal plane of graphene [22]. The particle size of the N, P-CDs ranged from 4.3 nm to 7.5 nm with an average particle size of about 6.21 nm.

Figure 2a shows the FTIR spectra of the N, P-CDs. The stretching vibrations of the N–H and O–H bonds are observed at 3390 cm^{−1} and 3170 cm^{−1}. The peak at 1670 cm^{−1} indicates the presence of stretching vibrations of the C=O or C=N and C=C structures in the carbon core skeleton of N, P-CDs [23]. A total of 1370 cm^{−1} corresponds to the C–N–C stretching vibration in the benzene ring, suggesting the possible presence of imine and piperazine structures in N, P-CDs [24]. The absorption peaks at 940–1260 cm^{−1} correspond to the P=O and P–O–R (R=alkyl) stretching vibrations [25]. The absorption peaks at 771 cm^{−1} and 607 cm^{−1} correspond to the bending vibration of C–H, which coincides with the out-of-plane bending vibration of the benzene ring C–H [26].

The chemical composition of the N, P-CDs was characterized using X-ray photoelectron spectroscopy. As shown in Figure 2b, the N, P-CDs show four peaks at 286.8 eV, 401.1 eV, 531.81 eV, and 133.39 eV. The atomic percentages of C, N, O, and P were 37.06%, 9.51%, 39.80%, and 16.63%, respectively. From the high-resolution spectra of C1s (Figure 2c), it can be seen that there are four chemical bonds in N, P-CDs, i.e., C=C/C–C (284.2 eV), C–N/C–P (285.7 eV), C–O (286.6 eV), and C=O (287.7 eV) [27,28].

High-resolution XPS spectra of N1s have three peaks at 399.2 eV, 400.1 eV, and 401.4 eV (Figure 2d), which correspond to pyridine N, pyrrole N, and graphite N, respectively [29]. The high-resolution spectra of O1s are 530.4 eV and 531.9 eV (Figure 2e), corresponding to the presence of both C–O and C=O forms of O [30]. The high-resolution XPS energy spectrum of P2p has two peaks at 132.9 eV and 134.1 eV (Figure 2f), indicating the presence of P=O and P–C/P–N chemical bonds [21].

To investigate the environmental stability of N, P–CDs, the effects of ionic strength, UV irradiation, and different pHs on the fluorescence intensity of N, P–CDs were investigated separately. As shown in Figure 3a, after 120 min of UV irradiation, the fluorescence intensity of N, P–CDs remained at 86.54% of its initial value, indicating that the optimized carbon dots have strong resistance to photobleaching and are suitable for large-scale preparation and storage. The fluorescence intensity of N, P–CDs under different salt concentration solutions (from 0 mol/L to 2 mol/L) was nearly the same, proving that the carbon dots have good salt tolerance, and that carbon dots have greater potential for biological applications. When N, P–CDs were dispersed in solutions with different pH values, the fluorescence intensity of the carbon dots remained almost unchanged at a pH of 1–12, showing excellent fluorescence stability. The intensity decreased at a pH of 13 and 14. This is probably due to the presence of more carboxyl groups on the surface of the carbon dots, which led to a chemical reaction on the surface of the carbon dots under strongly alkaline conditions, resulting in a weakening of their fluorescence intensity [31].

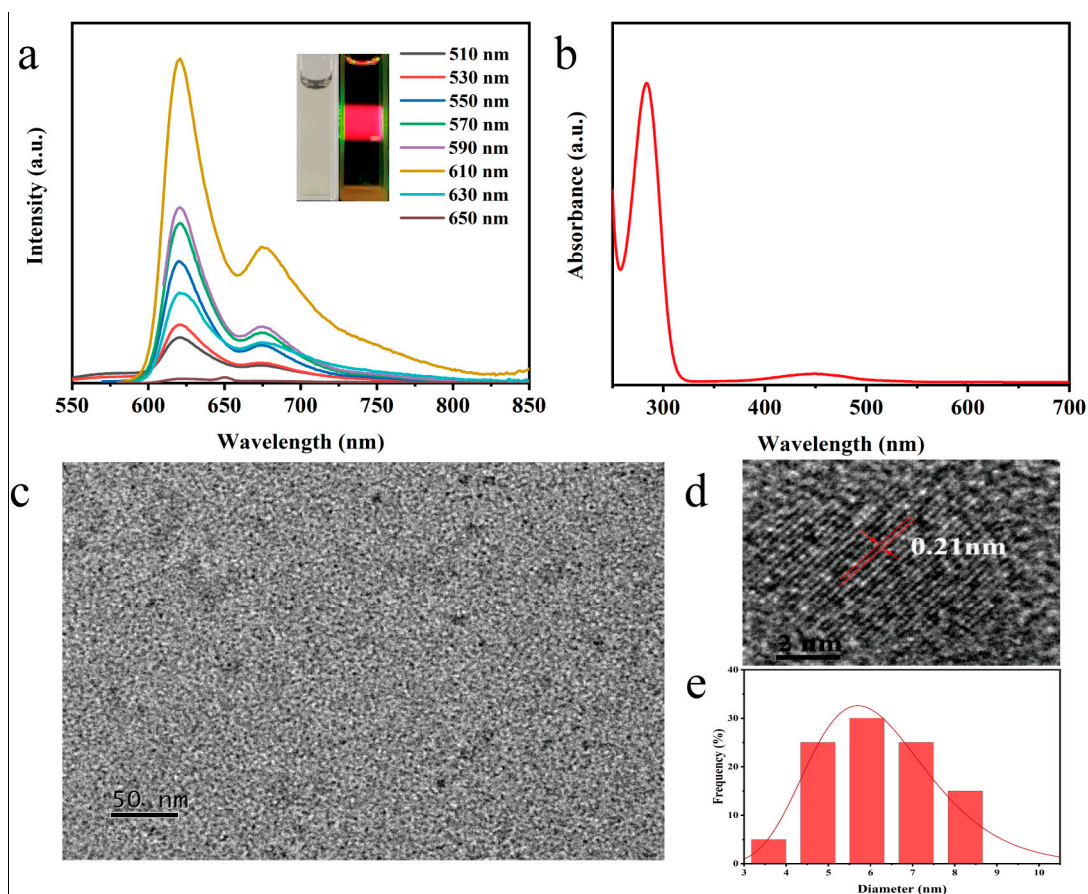


Figure 1. (a) Fluorescence spectra of N, P–CDs at different excitation wavelengths; inset shows the photograph of N, P–CDs under daylight and 530 nm excitation. (b) UV–vis absorption spectra of N, P–CDs. (c) TEM image of N, P–CDs. (d) HRTEM image. (e) Histogram of the size distribution of N, P–CDs.

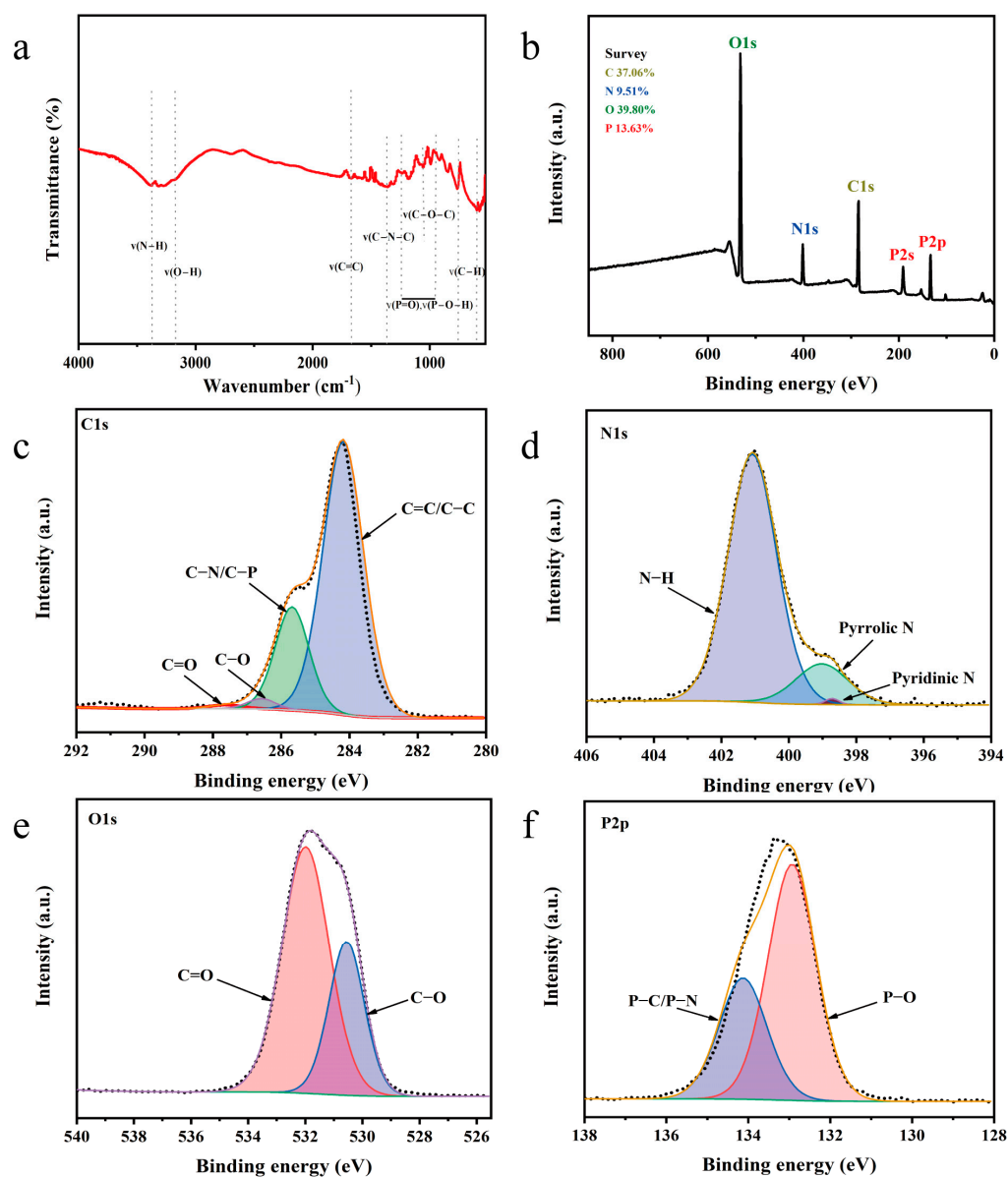


Figure 2. (a) FTIR spectra of N, P-CDs. XPS patterns of the (b) full scan, (c) C_{1s} scan, (d) N_{1s} scan, (e) O_{1s} scan, and (f) P_{2p} scan of N, P-CDs.

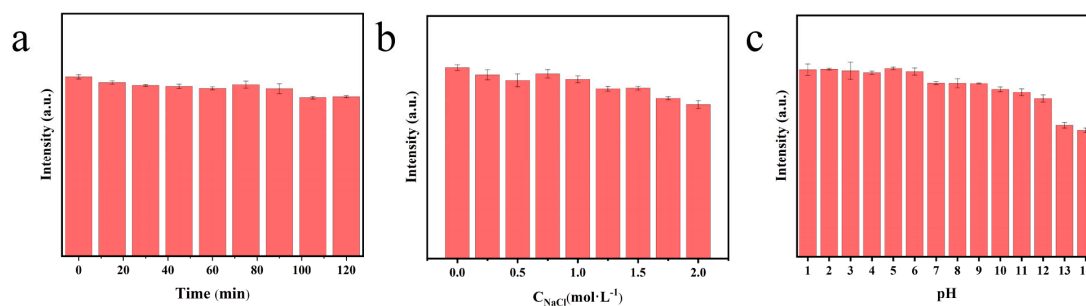


Figure 3. Stability of N, P-CDs. (a) Under UV light irradiation. (b) Under different concentrations of NaCl. (c) At different pHs.

3.2. Effect of N, P-CDs on the Growth of Water Spinach

Figure 4 reflects the growth of water spinach at different N, P-CD concentrations. We can see that at low concentrations of N, P-CDs, both treatments have a growth-promoting effect on water spinach, while at a concentration of 200 mg/L, growth inhibition is shown. As an edible vegetable, the leaves and stems of water spinach are the main part of the food, so it is particularly important to measure the parameters related to the thickness of the leaves and stems. Tables S1 and S2 show the values of the morphological indicators of water spinach. We found that under the two methods of leaf spraying and root spraying, the plant height, stem diameter, maximum functional leaf area, and the number of leaves of water spinach showed a trend of first increasing and then decreasing.

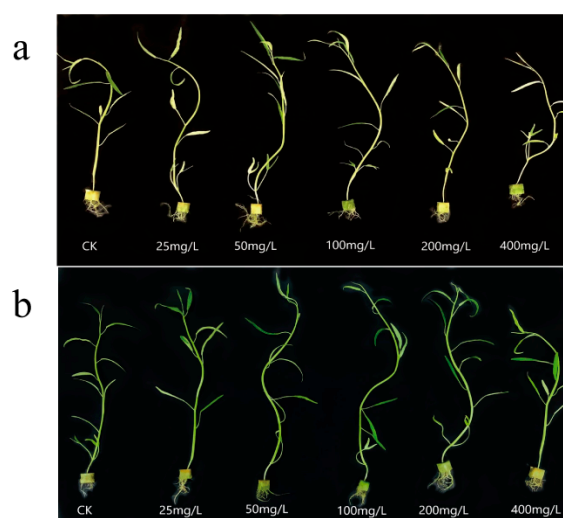


Figure 4. (a) Water spinach under leaf-spray treatment. (b) Water spinach under root-spray treatment.

Usually, the amount of plant growth is the main indicator to evaluate the growth status of a plant, and the plant's dry weight reflects the accumulation of organic matter in the plant. To investigate whether N, P-CDs can influence the extent of organic matter accumulation in water spinach, we carried out this research (Figure 5a–d). Compared to the control blank group, the fresh (dry) weight of the stem and leaf parts and the fresh (dry) weight of the root part values of water spinach treated with the leaf-spraying method (50 mg/L of N, P-CD solution) increased by 59.50% (59.03%) and 101.71% (64.78%), respectively ($p < 0.05$). Compared to the control blank group, the fresh (dry) weight of the stem and leaf parts and the fresh (dry) weight of the root part values of water spinach treated with the root-spraying method (100 mg/L of N, P-CD solution) increased by 90.37% (67.32%) and 104.91% (68.88%), respectively ($p < 0.05$). Taken together, the above experiments showed that the different cultivation methods were able to increase the dry weight of water spinach at low concentrations of N, P-CDs. The increase in the fresh weight of the stem and leaf parts of water spinach was much greater with the root-spraying method than with the leaf-spraying method. The difference in the dry weight increase between the two cultivation methods was not significant.

The anthocyanins, flavonoids, and total phenols in plants have free-radical scavenging, antioxidant, and detoxifying properties. Therefore, measuring the content of anthocyanins, flavonoids and total phenols in a plant can evaluate the nutritional quality of the plant. Figure 6a–c show the anthocyanin, total phenol, and flavonoid content of water spinach. Compared to the control blank group, the anthocyanin, total phenol, and flavonoid values of water spinach treated with the leaf-spraying method (50 mg/L of N, P-CD solution) increased by 70.79%, 57.78%, and 77.95%, respectively ($p < 0.05$). Compared to the control blank group, the anthocyanin, total phenol, and flavonoid values of water spinach

treated with the root-spraying method (100 mg/L of N, P-CD solution) increased by 85.49%, 23.45%, and 58.08%, respectively ($p < 0.05$).

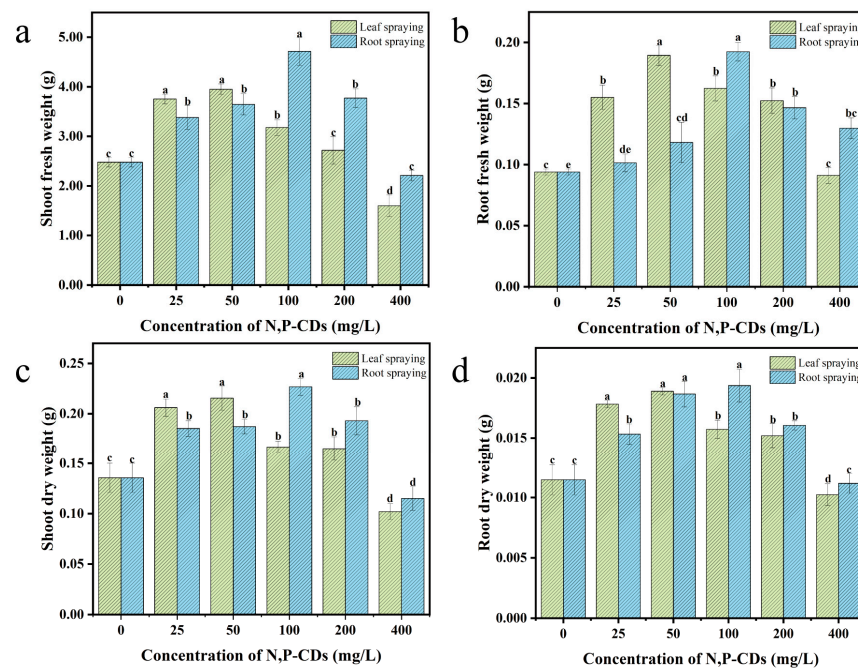


Figure 5. (a) Fresh weight of stems and the leaf of water spinach. (b) Fresh weight of roots of water spinach. (c) The dry weight of stems and the leaf of water spinach. (d) The dry weight of roots of water spinach. Different letters on the scale bar indicate significant differences for the respective parameters at $p < 0.05$.

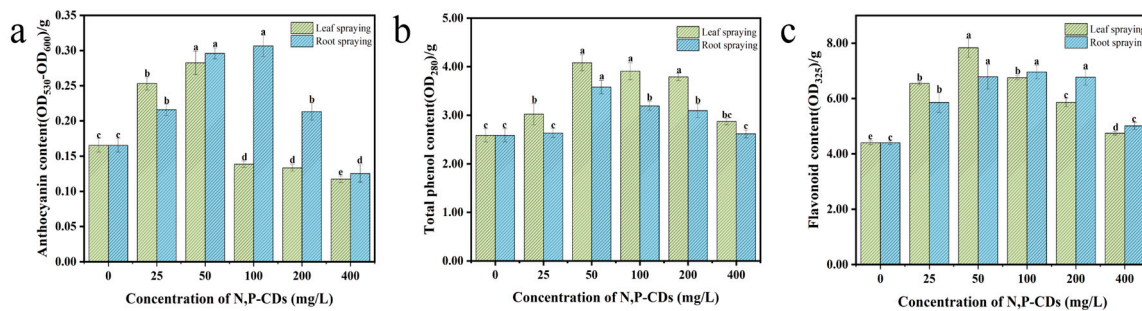


Figure 6. The content of (a) anthocyanins, (b) total phenols, and (c) flavonoids in water spinach. Different letters on the scale bar indicate significant differences for the respective parameters at $p < 0.05$.

Combined with the above experiments, we found that N, P-CDs were effective in enhancing the anthocyanin, total phenol, and flavonoid content of water spinach. It is known that phenylalanine can be converted into other metabolites such as phenols, anthocyanins, flavonoids, and isoflavones through various enzymatic reactions [32]. Phenylalanine ammonia-lyase (PAL) as a key enzyme in the phenylalanine metabolic pathway can influence the number of phenolic compounds produced from phenylalanine [33]. Anthocyanins are a type of flavonoid and have several reactions in common with flavonoids in their synthetic pathway [34]. The synthesis of flavonoids in plants is regulated by a combination of enzymes. However, the enzymes that mainly affect the reaction rate are chalcone synthase (CHS) and chalcone isomerase (CHI). The two enzymes affect the content of chalcone and naringenin and other substances, respectively, and the synthesis of anthocyanins in plants requires naringenin and other substances as precursors to synthesize [35]. The flavonoid and anthocyanin contents of water spinach showed approximately the same

trend in the experiment, and thus we propose the following mechanism: N, P-CDs can affect the activity of PAL and CHS, and the enhanced activity of PAL and CHS can increase the flavonoid and total phenolic contents of water spinach. In addition, we found that the experimental results obtained with water spinach cultivated by leaf spraying and root spraying were not the same, which was attributed to the different ways carbon dots were transported in the plant. When treated with root spraying, the presence of a large number of groups on the surface of the carbon dots causes a positive charge to be attached to their surface, creating an electrostatic attraction with the negative charge on the surface of the plant roots [36]. This promotes a large uptake of carbon dots at the root surface. The carbon dots that enter the plant's interior pass through the vascular system through the plant's roots, stems, and leaves and eventually reach the leaf veins [37]. During this transport process, some of the carbon dots are broken down by the roots, stems, and leaves of the plant, and the decomposition produces phytohormone analogs which have a growth-promoting effect on the plant [27]. However, when treated by leaf spraying, the carbon dots can enter the plant's leaf veins directly, avoiding the loss of carbon dots during transport.

3.3. Effect of N, P-CDs on the Photosynthetic Properties of Water Spinach

Photosynthetic pigments absorb and transmit light energy during photosynthesis in plants. The number of photosynthetic pigments greatly influences the photosynthetic rate of plants [38,39]. We measured the chlorophyll a, chlorophyll b, chlorophyll (a + b), and carotenoid contents in water spinach (Figure 7a,b). Compared to the control blank group, the chlorophyll a, chlorophyll b, chlorophyll (a + b), and carotenoids values of water spinach treated with the leaf-spraying method (50 mg/L of N, P-CD solution) increased by 18.84%, 26.61%, 20.67%, and 30.62%, respectively ($p < 0.05$). Compared to the control blank group, the chlorophyll a, chlorophyll b, chlorophyll (a + b), and carotenoids values of water spinach treated with the root-spraying method (100 mg/L of N, P-CD solution) increased by 38.17%, 38.67%, 38.29%, and 51.54%, respectively ($p < 0.05$).

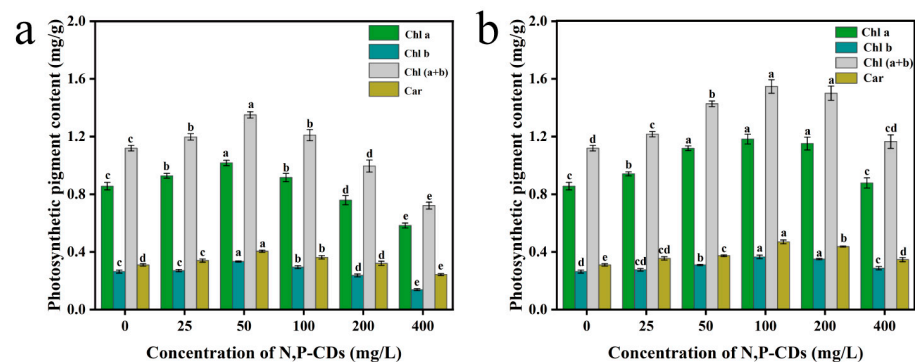


Figure 7. (a) The content of photosynthetic pigments in water spinach under leaf-spraying treatment. (b) The content of photosynthetic pigments in water spinach under root-spraying treatment. Different letters on the scale bar indicate significant differences for the respective parameters at $p < 0.05$.

Plants convert solar energy into chemical energy through photosynthesis and use it to synthesize organic matter for their growth, so the rate of photosynthesis reflects the extent of plant growth. To understand the effect of different methods on the photosynthetic parameters of water spinach, we measured the values of the net photosynthetic rate Pn, Gs, Ci, and Tr, as shown in Figure 8a–d. The experimental results showed that the Pn value of water spinach treated with the leaf-spraying method increased by 108.27% at 50 mg/L compared to the control group, which was a considerable increase. Compared to the control group, the values of Gs, Ci, and Tr increased by 46.61%, 40.99%, and 71.52% under a N, P-CD treatment of 50 mg/L, respectively, and all the values were different from the control group ($p < 0.05$). Compared to the control group, the Pn, Gs, Ci, and Tr values of

water spinach treated with the root–spraying method (100 mg/L of carbon dots solution) increased by 131.96%, 53.93%, 50.50%, and 88.66%, respectively. All the parameters of this group were different from the control group ($p < 0.05$).

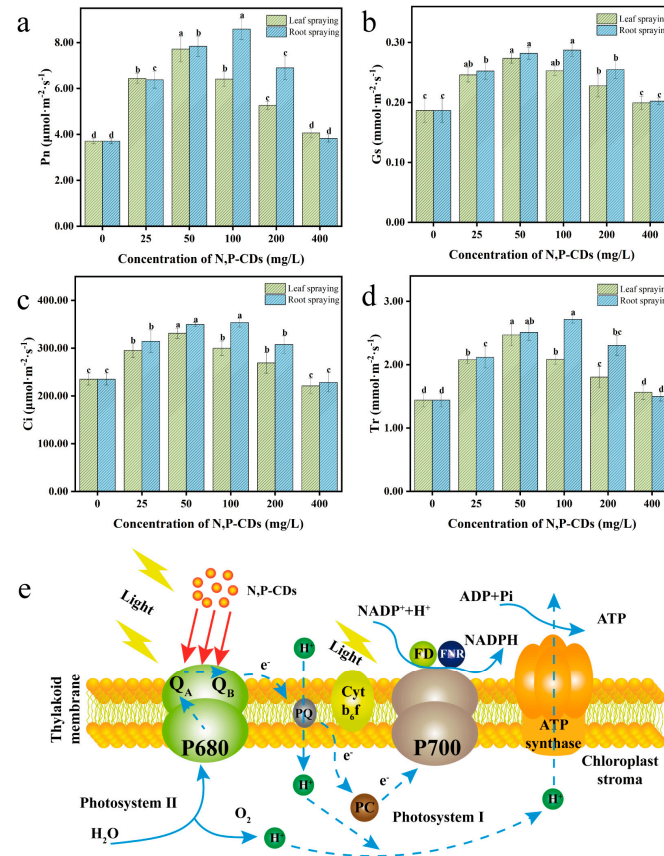


Figure 8. (a) Net photosynthetic rate, (b) stomatal conductance, (c) intercellular CO₂ concentration, (d) transpiration rate for water spinach. (e) Mechanism diagram illustrating how N, P–CDs boost the photosystem of plants. Different letters on the scale bar indicate significant differences for the respective parameters at $p < 0.05$.

4. Discussion

Chemical fertilizer is an indispensable material in agricultural production [40]. However, the use of fertilizer in actual production will increase the cost; meanwhile, residual fertilizer that cannot be absorbed and utilized by plants will enter the environment and adversely affect the ecosystem [41]. In contrast, carbon dots are environmentally friendly nanomaterials which are easy to prepare. In this research, we have explored the growth and photosynthesis of water spinach by using N, P–CDs with different methods during the growth of water spinach.

Photosynthetic pigments are molecules that can absorb and capture light, and their content reflects the strength of photosynthesis in plants [42]. Among them, chlorophyll, as an important photosynthetic pigment, can effectively absorb red and blue light [39,43]. Introducing N, P–CDs can increase the content of chlorophyll in water spinach, which is beneficial for it to absorb more light energy during photosynthesis [44]. This also reasonably explains why the net photosynthetic rate of water spinach increases after the introduction of N, P–CDs. In addition, the increase in the net photosynthetic rate led to a corresponding increase in the stomatal conductance of water spinach. The increase in Ci content in water spinach can be attributed to the entry of carbon dots into the plant, which is partially degraded by horseradish peroxidase (HRP) and H₂O₂ in the plant to produce CO₂ [27]. Studies have shown that plant water channel proteins can affect plant transpiration by

regulating internal plant water [45]. Considering that the carbon dots can activate the expression of genes encoding water channel proteins, we speculate that the increased Tr value of water spinach is related to the expression of genes encoding water channel proteins [23].

Photosynthesis is usually divided into two parts: the light reaction and the dark reaction. During the dark reaction, CO₂ is reduced to organic matter through the Calvin cycle, a process that requires the consumption of adenosine triphosphate (ATP) [46]. The light reaction provides nicotinamide adenine dinucleotide phosphate (NADPH) and ATP for the dark reaction [47]. Figure 8e shows the mechanism of how the N, P-CDs promote the plant photosynthesis process. N, P-CDs act as photosynthetic antennas during plant photosynthesis, i.e., they produce electrons by absorbing ultraviolet radiation from light and converting it to red light [48]. Photosynthetic electron transport occurs mainly through four macromolecular complexes, photosystem I (PSI), photosystem II (PSII), cytochrome b₆f complex (Cyt b₆f) and ATP synthase [49]. Electrons from N, P-CD fluorescence and those from water decomposition are transferred to P680 by antenna pigments and reaction center pigments capture, respectively, and then to plastoquinone (PQ) by Q_A-Q_B (primary and secondary quinone electron acceptors) [50]. The reduced-state PQ transfers electrons to Cyt b₆f, which releases protons into the membrane upon oxidation [51]. P700 provides electrons to reduce nicotinamide adenine dinucleotide phosphate (NADP⁺) to NADPH, and to maintain its own charge balance, obtains electrons from PQ. Water decomposition produces more protons, making a concentration difference between the two sides of the membrane, prompting ATP synthesis [52].

5. Conclusions

In summary, we have successfully synthesized novel kinds of N, P-CDs. The average particle size of this carbon dot is about 6.21 nm, and it can maintain high stability for a long time under UV light and other conditions. FTIR spectroscopy and XPS confirmed that it contains a large number of amino and hydroxyl structures, which give it excellent water solubility properties. The N, P-CDs were applied in the growth process of water spinach by root and leaf spraying. It was demonstrated that N, P-CDs were effectively absorbed by water spinach, enhanced the photosynthesis process by increasing the photosynthetic pigment content in the plant, and eventually promoted the growth of the plant. Also, we found that leaf spraying has a similar promotion effect with root spraying, yet it is more effective because of the more-efficient transport of N, P-CDs into the plant by leaf spraying. This work suggests that N, P-CDs provide a new avenue for future agricultural production applications.

Supplementary Materials: The following supporting information can be downloaded at: <https://www.mdpi.com/article/10.3390/sym15081532/s1>, Table S1: Effect of different concentrations of carbon dots on the mean values of plant height, stem thickness, maximum functional leaf area, and number of leaves of water spinach under the leaf spraying method; Table S2: Effect of different concentrations of carbon dots on the mean values of plant height, stem thickness, maximum functional leaf area, and number of leaves of water spinach under the root spraying method.

Author Contributions: F.Y., M.S. and X.C. experimented. F.Y. wrote the manuscript. X.L. contributed to the revision of the draft; Y.H., Z.T. and H.L. reviewed and edited the manuscript. All authors have read and agreed to the published version of the manuscript.

Funding: This work was supported by Huazhong Agricultural University/Agricultural Genomics Institute of Shenzhen Chinese Academy of Agricultural Sciences Cooperation Fund (SZYJY2022006), The Fundamental Research Funds for the Central Universities (Grant No. 2662020LXPY008, 2662022YLYJ010, 2662023LXPY006) and the Open Foundation of Hubei Key Laboratory of Optical Information and Pattern Recognition of Wuhan Institute of Technology (Grant No. 202103).

Institutional Review Board Statement: Not applicable.

Informed Consent Statement: Not applicable.

Data Availability Statement: The data presented in this study are available on request from the corresponding author.

Conflicts of Interest: No potential conflict of interest were reported by the authors.

References

1. Kalala, G.; Kambashi, B.; Everaert, N.; Beckers, Y.; Richel, A.; Pachikian, B.; Neyrinck, A.M.; Delzenne, N.M.; Bindelle, J. Characterization of fructans and dietary fibre profiles in raw and steamed vegetables. *Int. J. Food Sci. Nutr.* **2017**, *69*, 682–689.
2. Calatayud, M.; Abbeele, P.V.D.; Ghyselinck, J.; Marzorati, M.; Rohs, E.; Birkett, A. Comparative Effect of 22 Dietary Sources of Fiber on Gut Microbiota of Healthy Humans In Vitro. *Front. Nutr.* **2021**, *8*, 700571.
3. Barbosa, C.L.; Brettschneider, A.-K.; Haftenberger, M.; Lehmann, F.; Richter, A.; Mensink, G.B. Food and nutrient intake of children and adolescents living in Germany: Results from EsKiMo II. *Proc. Nutr. Soc.* **2020**, *79*, OCE2.
4. Wang, A.; Luo, J.; Zhang, T.; Zhang, D. Dietary Vitamin C and Vitamin C Derived from Vegetables Are Inversely Associated with the Risk of Depressive Symptoms among the General Population. *Antioxidants* **2021**, *10*, 1984. [\[CrossRef\]](#)
5. Sivadas, S.; Mohanty, A.K.; Rajesh, S.; Muthuvel, S.K.; Vasanthi, H.R. Molecular modelling and biological evaluation of phyto-molecules as potential activators of gluconolactone oxidase (GULO). *J. Biomol. Struct. Dyn.* **2023**, *3*, 1–13.
6. Kathi, S.; Laza, H.; Singh, S.; Thompson, L.; Li, W.; Simpson, C. Increasing vitamin C through agronomic biofortification of arugula microgreens. *Sci. Rep.* **2022**, *12*, 13093.
7. Bidar, G.; Pelfrène, A.; Schwartz, C.; Waterlot, C.; Sahmer, K.; Marot, F.; Douay, F. Urban kitchen gardens: Effect of the soil contamination and parameters on the trace element accumulation in vegetables—A review. *Sci. Total Environ.* **2020**, *738*, 139569.
8. Manzoor, J.; Sharma, M.; Wani, K.A. Heavy metals in vegetables and their impact on the nutrient quality of vegetables: A review. *J. Plant Nutr.* **2018**, *41*, 1744–1763.
9. Scharff, L.B.; Saltenis, V.L.R.; Jensen, P.E.; Baekelandt, A.; Burgess, A.J.; Burow, M.; Ceriotti, A.; Cohan, J.; Geu-Flores, F.; Halkier, B.A.; et al. Prospects to improve the nutritional quality of crops. *Food Energy Secur.* **2021**, *11*, e327.
10. Jusuf, B.N.; Sambudi, N.S.; Isnaeni; Samsuri, S. Microwave-assisted synthesis of carbon dots from eggshell membrane ashes by using sodium hydroxide and their usage for degradation of methylene blue. *J. Environ. Chem. Eng.* **2018**, *6*, 7426–7433.
11. Cao, Y.; Fan, D.; Lin, S.; Mu, L.; Ng, F.T.; Pan, Q. Phase change materials based on comb-like polynorbornenes and octadecylamine-functionalized graphene oxide nanosheets for thermal energy storage. *Chem. Eng. J.* **2020**, *389*, 124318.
12. Xia, C.; Zhu, S.; Feng, T.; Yang, M.; Yang, B. Evolution and Synthesis of Carbon Dots: From Carbon Dots to Carbonized Polymer Dots. *Adv. Sci.* **2019**, *6*, 1901316.
13. Sawalha, S.; Silvestri, A.; Criado, A.; Bettini, S.; Prato, M.; Valli, L. Tailoring the sensing abilities of carbon nanodots obtained from olive solid wastes. *Carbon* **2020**, *167*, 696–708.
14. Hallaji, Z.; Bagheri, Z.; Tavassoli, Z.; Ranjbar, B. Fluorescent carbon dot as an optical amplifier in modern agriculture. *Sustain. Mater. Technol.* **2022**, *34*, e00493.
15. Zhang, M.; Hu, L.; Wang, H.; Song, Y.; Liu, Y.; Li, H.; Shao, M.; Huang, H.; Kang, Z. One-step hydrothermal synthesis of chiral carbon dots and their effects on mung bean plant growth. *Nanoscale* **2018**, *10*, 12734–12742.
16. Su, L.-X.; Ma, X.-L.; Zhao, K.-K.; Shen, C.-L.; Lou, Q.; Yin, D.-M.; Shan, C.-X. Carbon Nanodots for Enhancing the Stress Resistance of Peanut Plants. *ACS Omega* **2018**, *3*, 17770–17777. [\[CrossRef\]](#)
17. Amarasinghe, T.; Madhusa, C.; Munaweera, I.; Kottegoda, N. Review on Mechanisms of Phosphate Solubilization in Rock Phosphate Fertilizer. *Commun. Soil Sci. Plant Anal.* **2022**, *53*, 944–960. [\[CrossRef\]](#)
18. Pan, X.; Fu, F.; Xie, Z.; Li, W.; Yang, X.; Kang, Y.; Qu, S.; Zheng, Y.; Li, Q.; Zhang, H.; et al. Light-nutrition coupling effect of degradable fluorescent carbon dots on lettuce. *Environ. Sci. Nano* **2023**, *10*, 539–551.
19. Krein, D.D.C.; Rosseto, M.; Cemin, F.; Massuda, L.A.; Dettmer, A. Recent trends and technologies for reduced environmental impacts of fertilizers: A review. *Int. J. Environ. Sci. Technol.* **2023**, 1–16. [\[CrossRef\]](#)
20. Cao, J.; Jiang, W.; Zhao, Y. *Postharvest Physiological and Biochemical Experimental Guidance for Fruits and Vegetables*; China Light Industry Press: Beijing, China, 2007; pp. 38–49.
21. Yu, S.-J.; Lu, S.-Y.; Tan, D.-F.; Zhu, Y.-F. Nitrogen and phosphorus co-doped carbon dots for developing highly flame retardant poly (vinyl alcohol) composite films. *Eur. Polym. J.* **2021**, *164*, 110970.
22. Perikala, M.; Bhardwaj, A. Engineering Photo-Luminescent Centers of Carbon Dots to Achieve Higher Quantum Yields. *ACS Appl. Electron. Mater.* **2020**, *2*, 2470–2478. [\[CrossRef\]](#)
23. Kou, E.; Yao, Y.; Yang, X.; Song, S.; Li, W.; Kang, Y.; Qu, S.; Dong, R.; Pan, X.; Li, D.; et al. Regulation Mechanisms of Carbon Dots in the Development of Lettuce and Tomato. *ACS Sustain. Chem. Eng.* **2021**, *9*, 944–953. [\[CrossRef\]](#)
24. Ju, Y.J.; Li, N.; Liu, S.G.; Liang, J.Y.; Gao, X.; Fan, Y.Z.; Li, N.B. Proton-controlled synthesis of red-emitting carbon dots and application for hematin detection in human erythrocytes. *Anal. Bioanal. Chem.* **2019**, *411*, 1159–1167. [\[CrossRef\]](#) [\[PubMed\]](#)
25. Zhao, D.; Zhang, Z.; Liu, X.; Zhang, R.; Xiao, X. Rapid and low-temperature synthesis of N, P co-doped yellow emitting carbon dots and their applications as antibacterial agent and detection probe to Sudan Red I. *Mater. Sci. Eng. C* **2020**, *119*, 111468.
26. Li, Y.; Pan, X.; Xu, X.; Wu, Y.; Zhuang, J.; Zhang, X.; Zhang, H.; Lei, B.; Hu, C.; Liu, Y. Carbon dots as light converter for plant photosynthesis: Augmenting light coverage and quantum yield effect. *J. Hazard. Mater.* **2020**, *410*, 124534.

27. Shao, D.; Zhu, W.; Xin, G.; Lian, J.; Sawyer, S. Inorganic vacancy-ordered perovskite Cs₂SnCl₆:Bi/GaN heterojunction photodiode for narrowband, visible-blind UV detection. *Appl. Phys. Lett.* **2019**, *115*, 121106.
28. Fan, H.; Lv, J.; Chen, W.; Dong, X.; Bian, W. Preparation of nitrogen and phosphorus co-doped carbon dots and its application for morin detection. *Chem. Res. Appl.* **2018**, *30*, 577–582.
29. Chen, J.; Wei, J.-S.; Zhang, P.; Niu, X.-Q.; Zhao, W.; Zhu, Z.-Y.; Ding, H.; Xiong, H.-M. Red-Emissive Carbon Dots for Fingerprints Detection by Spray Method: Coffee Ring Effect and Unquenched Fluorescence in Drying Process. *ACS Appl. Mater. Interfaces* **2017**, *9*, 18429–18433.
30. Li, L.; Dong, T. Photoluminescence tuning in carbon dots: Surface passivation or/and functionalization, heteroatom doping. *J. Mater. Chem. C* **2018**, *6*, 7944–7970.
31. Dong, G.; Yu-Liang, Z.; Jing, S.; Hong-Jun, F. One-Step Synthesis of Specific pH-responsive Carbon Quantum Dots and Their Luminescence Mechanism. *J. Inorg. Mater.* **2019**, *34*, 1309–1315.
32. Hu, W.; Sarengaowa; Guan, Y.; Feng, K. Biosynthesis of Phenolic Compounds and Antioxidant Activity in Fresh-Cut Fruits and Vegetables. *Front. Microbiol.* **2022**, *13*, 906069. [[CrossRef](#)] [[PubMed](#)]
33. Christopoulos, M.V.; Tsantili, E. Participation of phenylalanine ammonia-lyase (PAL) in increased phenolic compounds in fresh cold stressed walnut (*Juglans regia* L.) kernels. *Postharvest Biol. Technol.* **2015**, *104*, 17–25.
34. Sunil, L.; Shetty, N.P. Biosynthesis and regulation of anthocyanin pathway genes. *Appl. Microbiol. Biotechnol.* **2022**, *106*, 1783–1798. [[CrossRef](#)] [[PubMed](#)]
35. Liu, W.; Feng, Y.; Yu, S.; Fan, Z.; Li, X.; Li, J.; Yin, H. The Flavonoid Biosynthesis Network in Plants. *Int. J. Mol. Sci.* **2021**, *22*, 12824. [[CrossRef](#)]
36. Lu, H.-L.; Nkoh, J.N.; Baquy, M.A.-A.; Dong, G.; Li, J.-Y.; Xu, R.-K. Plants alter surface charge and functional groups of their roots to adapt to acidic soil conditions. *Environ. Pollut.* **2020**, *267*, 115590. [[PubMed](#)]
37. Li, W.; Zheng, Y.; Zhang, H.; Liu, Z.; Su, W.; Chen, S.; Liu, Y.; Zhuang, J.; Lei, B. Phytotoxicity, Uptake, and Translocation of Fluorescent Carbon Dots in Mung Bean Plants. *ACS Appl. Mater. Interfaces* **2016**, *8*, 19939–19945.
38. Simkin, A.J.; Kapoor, L.; Doss, C.G.P.; Hofmann, T.A.; Lawson, T.; Ramamoorthy, S. The role of photosynthesis related pigments in light harvesting, photoprotection and enhancement of photosynthetic yield in planta. *Photosynth. Res.* **2022**, *152*, 23–42.
39. Khatri, K.; Rathore, M.S. Salt and osmotic stress-induced changes in physio-chemical responses, PSII photochemistry and chlorophyll a fluorescence in peanut. *Plant Stress* **2022**, *3*, 100063.
40. Liao, C.; Nolte, K.; Brown, D.G.; Lay, J.; Agrawal, A. The carbon cost of agricultural production in the global land rush. *Glob. Environ. Chang.* **2023**, *80*, 102679.
41. Cánovas, C.R.; Macías, F.; Pérez-López, R.; Basallote, M.D.; Millán-Becerro, R. Valorization of wastes from the fertilizer industry: Current status and future trends. *J. Clean. Prod.* **2018**, *174*, 678–690.
42. Kreslavski, V.D.; Los, D.A.; Schmitt, F.-J.; Zharmukhamedov, S.K.; Kuznetsov, V.V.; Allakhverdiev, S.I. The impact of the phytochromes on photosynthetic processes. *Biochim. Biophys. Acta (BBA)-Bioenerg.* **2018**, *1859*, 400–408.
43. Mascoli, V.; Bersanini, L.; Croce, R. Far-red absorption and light-use efficiency trade-offs in chlorophyll f photosynthesis. *Nat. Plants* **2020**, *6*, 1044–1053. [[CrossRef](#)] [[PubMed](#)]
44. Li, W.; Wu, S.; Zhang, H.; Zhang, X.; Zhuang, J.; Hu, C.; Liu, Y.; Lei, B.; Ma, L.; Wang, X. Enhanced Biological Photosynthetic Efficiency Using Light-Harvesting Engineering with Dual-Emissive Carbon Dots. *Adv. Funct. Mater.* **2018**, *28*, 4004.
45. Maurel, C.; Verdoucq, L.; Rodrigues, O. Aquaporins and plant transpiration. *Plant Cell Environ.* **2016**, *39*, 2580–2587. [[PubMed](#)]
46. Bellasio, C. A generalised dynamic model of leaf-level C₃ photosynthesis combining light and dark reactions with stomatal behaviour. *Photosynth. Res.* **2018**, *141*, 99–118. [[PubMed](#)]
47. Hitchcock, A.; Hunter, C.N.; Sobotka, R.; Komenda, J.; Dann, M.; Leister, D. Redesigning the photosynthetic light reactions to enhance photosynthesis—The *PhotoRedesign* consortium. *Plant J.* **2021**, *109*, 23–34. [[CrossRef](#)]
48. Guirguis, A.; Yang, W.; Conlan, X.A.; Kong, L.; Cahill, D.M.; Wang, Y. Boosting Plant Photosynthesis with Carbon Dots: A Critical Review of Performance and Prospects. *Small* **2023**, *6*, e2300671.
49. Zhao, L.-S.; Huokko, T.; Wilson, S.; Simpson, D.M.; Wang, Q.; Ruban, A.V.; Mullineaux, C.W.; Zhang, Y.-Z.; Liu, L.-N. Structural variability, coordination and adaptation of a native photosynthetic machinery. *Nat. Plants* **2020**, *6*, 869–882. [[CrossRef](#)]
50. Stefanov, M.A.; Rashkov, G.D.; Apostolova, E.L. Assessment of the Photosynthetic Apparatus Functions by Chlorophyll Fluorescence and P₇₀₀ Absorbance in C₃ and C₄ Plants under Physiological Conditions and under Salt Stress. *Int. J. Mol. Sci.* **2022**, *23*, 3768.
51. Borisova-Mubarakshina, M.M.; Vetoshkina, D.V.; Ivanov, B.N. Antioxidant and signaling functions of the plastoquinone pool in higher plants. *Physiol. Plant.* **2019**, *166*, 181–198.
52. Lee, K.Y.; Park, S.J.; Lee, K.A.; Kim, S.H.; Kim, H.; Meroz, Y.; Shin, K. Photosynthetic artificial organelles sustain and control ATP-dependent reactions in a protocellular system. *Nat. Biotechnol.* **2018**, *36*, 530–535. [[CrossRef](#)] [[PubMed](#)]

Disclaimer/Publisher’s Note: The statements, opinions and data contained in all publications are solely those of the individual author(s) and contributor(s) and not of MDPI and/or the editor(s). MDPI and/or the editor(s) disclaim responsibility for any injury to people or property resulting from any ideas, methods, instructions or products referred to in the content.